Special Issue on Selected Emerging Trends in Terahertz Science and Technology

THz Communications and the Demonstration in the ThoR–Backhaul Link

Thomas Kürner, *Fellow, IEEE*, Ralf-Peter Braun, Guillaume Ducournau, *Member, IEEE*, Uwe Hellrung, Akihiko Hirata, *Senior Member, IEEE*, Shintaro Hisatake, *Member, IEEE*, Laurenz John, Bo Kum Jung, Ingmar Kallfass, *Member, IEEE*, Tetsuya Kawanishi, *Fellow, IEEE*, Keitarou Kondou, Yigal Leiba, Bruce Napier, Ran Timar, Alexandre Renau, Peter Schlegel, Pascal Szriftgiser, Axel Tessmann, and Dominik Wrana, *Graduate Student Member, IEEE*

***Abstract*—This article provides a brief overview on THz communications and subsequently focuses on the application of 300 GHz backhaul and fronthaul links. The fundamentals, planning, and software simulation approaches as well as the realized bidirectional 300 GHz demonstrator built within the Horizon 2020 joint EU-Japan project ThoR are described. The ThoR demonstrator uses off-the-shelf modems for network connections and baseband processing, RF front-ends based on InGaAs mHEMT technology and a spurious-free/low-phase noise photonic solution for LO generation. With the ThoR set-up, a net data rate of 2 × 20 Gbps over a distance of 150 m using a total instantaneous bandwidth of 8.64 GHz has been demonstrated. It is also shown that the IEEE Std 802.15.3-2023 protocol works correctly for this application.**

***Index Terms*—Backhaul links, demonstration, IEEE Std 802.15.3-2023, THz communications.**

Manuscript received 14 February 2024; revised 8 May 2024; accepted 28 May 2024. Date of publication 17 June 2024; date of current version 5 September 2024. This work was supported in part by the Horizon 2020, the European Union's Framework Programme for Research and Innovation under Grant 814523, in part by the National Institute of Information and Communications Technology in Japan (NICT) through ThoR, in part by NICT, Japan, for the development of automatic fronthaul deployment algorithm and the outdoor radio units under Grant JPJ012368C04301, in part by JST ASPIRE for outdoor units that are planned to be used for EU-Japan collaboration under Grant JPMJAP2324, in part by CPER Wavetech, which is supported by the Ministry of Higher Education and Research, the Hautsde- France Regional Council, Lille European Metropolis (MEL), the Institute of Physics of the French National Centre for Scientific Research (CNRS), and the European Regional Development Fund (ERDF) for THz testbed. *(Corresponding author: Thomas Kürner.)*

Thomas Kürner, Uwe Hellrung, Bo Kum Jung, and Peter Schlegel are with the Institut für Nachrichtentechnik, Technische Universität Braunschweig, D-38106 Braunschweig, Germany (e-mail: t.kuerner@tu-braunschweig.de; uwe.hellrung@tu-braunschweig.de; bo.jung@tu-braunschweig.de; p.schlegel@tu-braunschweig.de).

Ralf-Peter Braun was with the Deutsche Telekom AG, Berlin, Germany. He is now with the Orbit GmbH, 53175 Bonn, Germany (e-mail: ralf-peter.braun@orbit.de).

Guillaume Ducournau and Alexandre Renau are with the CNRS, Institut d'Electronique, Microelectronique et Nanotechnologie, IEMN, Univ. Lille, F-59000 Lille, France (e-mail: guillaume.ducournau@univ-lille.fr).

Akihiko Hirata is with the Faculty of Engineering, Chiba Institute of Technology, Narashino-shi 2750016, Japan (e-mail: hirata.akihiko@p.chibakoudai.jp).

Shintaro Hisatake is with the Electrical and Energy System Engineering Division, Faculty of Engineering, Gifu University, Gifu 501-1193, Japan (e-mail: hisatake.shintaro.f4@f.gifu-u.ac.jp).

Laurenz John and Axel Tessmann are with the Fraunhofer IAF, Fraunhofer Institute for Applied Solid State Physics, D-79108 Freiburg, Germany (e-mail: laurenz.john@iaf.fraunhofer.de; axel.tessmann@iaf.fraunhofer.de).

Ingmar Kallfass and Dominik Wrana are with the Institute of Robust Power Semiconductor Systems, University of Stuttgart, 70569 Stuttgart, Germany (e-mail: ingmar.kallfass@ilh.uni-stuttgart.de; dominik.wrana@ilh.uni-stuttgart.de).

Tetsuya Kawanishi is with the Faculty of Science and Engineering, Waseda University, Shinjuku-ku, Tokyo 169-8555, Japan (e-mail: kawanishi@waseda.jp).

Keitarou Kondou is with the HRCP Research and Development Partnership, Tokyo 105-0004, Japan (e-mail: keitarou.kondou@hrcp.jp).

Yigal Leiba was with the Siklu Communications Ltd., Petach Tikva, Israel. He is now with the Genopore Ltd, Yavne 8122004, Israel (e-mail: yigalle@genopore.com).

Bruce Napier is with the Vivid Components Germany UG, D-33102 Paderborn, Germany (e-mail: bruce@vividcomponents.co.uk).

Ran Timar was with the Siklu Communications Ltd., Petach Tikva, Israel. He is now with the Ceragon Networks, Tel Aviv 5336005, Israel (e-mail: rant@ceragon.com).

Pascal Szriftgiser is with the CNRS, Laboratoire de Physique des Lasers, Atomes et Molécules, PhLAM, Univ. Lille, F-59000 Lille, France (e-mail: pascal.szriftgiser@univ-lille.fr).

Color versions of one or more figures in this article are available at https://doi.org/10.1109/TTHZ.2024.3415480.

Digital Object Identifier 10.1109/TTHZ.2024.3415480

I. Introduction

THZ communications have been a subject of research for several decades. It is seen as a means to realize transmission of several 10 s of Gbps with the potential to achieve 1 Tbps [1] using spectrum beyond 275 GHz, where currently no spectrum allocation exists. Early concepts were published by Piesiewicz et al. [2] and by [3]. The main focus in research on THz communications has been on carrier frequencies around 300 GHz using both photonic and electronic means to generate and detect THz signals [1]. Since then the development of semiconductor technology has evolved enabling a significant number of hardware demonstrations in laboratory environments. For example, Koenig et al. [4] demonstrated in 2013, a wireless data transmission of 100 Gbps over a distance of 20 m, which marked a world record at that time. Electronic beam-steering at 300 GHz was demonstrated in 2016 within the German project TERAPAN ("THz Communications for the Next Generation of Wireless Personal Area Networks") [5]. Due to the harsh propagation conditions at around 300 GHz, see e.g., [2], high-gain antenna concepts are required favoring applications with fixed antenna directions at both ends of the link. These conditions can be found in wireless fronthaul or backhaul links connecting base stations in cellular networks. Wireless links for backhaul/fronthaul

wireless connections might be required in ultra-dense fifth and sixth generation (5 G/6 G) cellular networks in order to meet the explosive growth of mobile traffic. Initial demonstrations of backhaul links operating at 240 GHz and beyond have been reported for example by Kallfass et al. [6] and Castro et al. [7]. In parallel to advances in semiconductor technologies, IEEE 802 published a first wireless standard targeting fixed point-to-point applications around 300 GHz in 2017 [8]. These developments set the scene for building the first bi-directional 300 GHz backhaul demonstrator enabling the transmission of real data [9] within the Horizon 2020 joint EU-Japan project ThoR ("TeraHertz end-to-end wireless systems supporting ultra-high data Rate applications"). This article focuses on the application of 300 GHz backhaul links. The article includes both a survey on the background and basics for THz communications in general and THz backhaul links specifically and elaborates on the novel aspects covered by the ThoR demonstrator. The latter comprises especially phase noise aspects of the photonic LO and the demonstrator itself as well as the results achieved with the ThoR demonstrator. While state-of-the-art demonstrators have been using laboratory equipment, the ThoR demonstrator aims at demonstrating for the first time a bi-directional full end-to-end demonstration with real-time-capable transparent transmission of Ethernet data of a 300-GHz P2P (point-to-point) link with a real-world-relevant link distance in excess of 100 m. The rest of this article is organized as follows: Section II will give a brief overview of the status of regulation and standardization followed by a brief description of the relevant propagation phenomena in Section III. Methods to characterize the required antennas are described in the subsequent Section IV. Section V introduces the RF hardware technology used in ThoR. Section VI includes the simulation and planning aspects of 300 GHz backhaul links. The demonstrator set-up and the results are provided in Section VII. Finally, Section VIII concludes this article.

II. THz Regulation and Standards

The global operation of wireless communication systems requires 1) the availability of spectrum and 2) the existence of wireless standards.

The availability of spectrum is ruled by the radio regulations, which are revised about every 4 years at the World Radiocommunications Conference (WRC). As a result of WRC-19, the 2020 edition of the Radio Regulations (RR) [10] includes 160 GHz of spectrum, which has been either allocated (252–275 GHz) or identified (a total of 137 GHz between 275 GHz and 450 GHz) for the use by mobile and fixed service, which are the ITU-R (International Telecommunications Union Radio Communications Sector) services relevant for THz communications. Another 33 GHz of spectrum between 296 and 368 GHz, have not been identified for the use by mobile and fixed service and might be used under strict conditions discussed in footnote FN 5.656 of the RR. As a result of the WRC-23 [11] agenda items for the WRC-27 and WRC-31 relevant for THz communications have been decided. At WRC-27, the allocation and identification of spectrum for radio location service, which includes also radar applications, will be discussed. This will touch on THz communications by the requirement to perform sharing studies and by the fact that joint sensing and communication applications are also discussed [12] in the context of THz, integrating for example communications and radar. At WRC-31 the allocation of spectrum between 275 and 325 GHz for all services of interest for this frequency band will be discussed. A more detailed study on the regulatory situation for all spectrum above 100 GHz has been made by the ETSI (European Telecommunications Standards Institute) Industry Specification Group (ISG) THz [13].

IEEE Std 802.15.3d-2017 [8] is the first wireless standard for carrier frequencies between 252 and 321 GHz targeting fixed wireless applications. The standard defines eight different bandwidths between 2.16 and 69.12 GHz, all of them multiples of 2.16 GHz. Furthermore, six single carrier modulation schemes plus OOK (ON-OFF Keying) modulation and three forward error correction (FEC) schemes have been defined. A brief overview of the basic features can be found, for example, in [14]. In 2023, the revised standard IEEE 802.15.3-2023 [15] was approved. The new features of the revised standard are the extension of carrier frequencies, including now all spectrum up to 450 GHz identified by WRC-19, to new Amplitude-Phase Shift Keying (APSK) modulation schemes as well as a long RIFS (Retransmisison Interframe Spacing), which is is required to enable the operation of longer distances between the two receivers. The minimum time interval between the retransmission of packets is determined by the round-trip time between transmitter and receiver. In IEEE Std 802.15.3e-2017, the targeted application assumed short distances with a few centimeters with RIFS covering only the corresponding short round-trip delay, up to several tens of meters at most. To enable operation with distances between Tx and Rx of up to 10 km an optional long version of the RIFS has been introduced. The latter changes have been triggered by findings in ThoR and were implemented in the chipset used in the ThoR demonstrations, which therefore complies with IEEE Std 802.15.3-2023, although it was performed back in 2022.

THz communications are now also seen as a potential component of and might be part of standardization activities in 3GPP (3rd Partnership Project). This has trigged prestandardisation activities at ETSI, which has established the ETSI ISG THz [16]. One of the first outcomes of these activities is a group report on the "Identification of Use Cases for THz Communication Systems" [17], which covers 19 different use cases that can be supported by THz communications and sensing systems and includes also a summary of requirements for these use cases.

III. THz Propagation Channel

The properties of the propagation channel at THz frequencies differ significantly from the channel at lower frequencies. The phenomena that are of particular interest are the following.

1) The free space path loss according to the Friis equation is high, resulting for example in 122 dB for a link distance of 100 m at 300 GHz. In order to mitigate this high path loss, high-gain antennas are required.

2) Atmospheric attenuation due to gaseous absorption, water vapor, or precipitation causes additional loss especially for longer distances [18]. This makes 300 GHz backhaul links sensitive to weather conditions [19] [20], [21]. In particular, attenuation due to heavy rainfall, which may even cause line disconnections during local downpours, needs to be taken into account in the design of wireless links.
3) The high diffraction loss observed at THz frequencies requires the existence of a line-of-sight connection between both ends of the link, or so-called obstructed line-of-sight (OLOS), where the communication takes places via reflection or scattering [2].
4) In the design of 300 GHz band wireless links, reflections may occur or might be even required to enable OLOS links. Therefore experimental data on reflectance and transmittance of building materials in the 300 GHz band is required. In [22], e.g., terahertz time-domain spectroscopy (THz-TDS) has been applied to obtain the complex permittivity of building materials, glass, concrete, and granite from 200 to 500 GHz. This data can be used in simulations, see e.g., Section VI.
5) The small wavelength, less than 1 mm for carrier frequencies beyond 300 GHz, causes significant scattering due to surface roughness [23]. A recent measurement campaign on a large number of building materials including rough surfaces and layer materials has been published by Taleb et al. [24].

A good overview of relevant propagation phenomena, their characterization by measurements as well as channel and propagation models and their application to complex environments can be found, for example, in [1] and [25]. For backhaul applications, the effect of atmospheric attenuation is the most relevant one. A detailed analysis of this effect related to the actual demonstration is included in Section VII.

IV. THz Antennas and Their Characterization

Antennas with a high gain of approximately 40–50 dBi are being considered for use in THz backhaul/fronthaul applications to overcome the large propagation loss. The radiation pattern characterization is required not only for the link design, but also for the frequency sharing with other applications. The methods of antenna radiation pattern characterization can be broadly classified into three: direct far-field measurement (FFM), compact antenna test range (CATR), and near-field measurement (NFM) [26]. The FF region is inversely proportional to the wavelength. The CATR is a method for obtaining the far-field pattern through Fourier transformation using concave mirrors and similar devices. For short-wavelength terahertz waves, it is challenging to manufacture large concave mirrors with high precision. At a frequency of 300 GHz, the far-field region of such high-gain antennas is located several tens of meters away, making direct evaluation of the far-field challenging. In the ThoR project, it was confirmed that the far-field evaluation results obtained via photonics-based near-field Measurement (NFM) for relatively low-gain antennas, which are capable of direct far-field measurements, agreed well with the direct measurement results. This result shows that the photonics-based NFM will be a useful solution in the design of terahertz wireless backhaul and fronthaul links that utilize high-gain antennas.

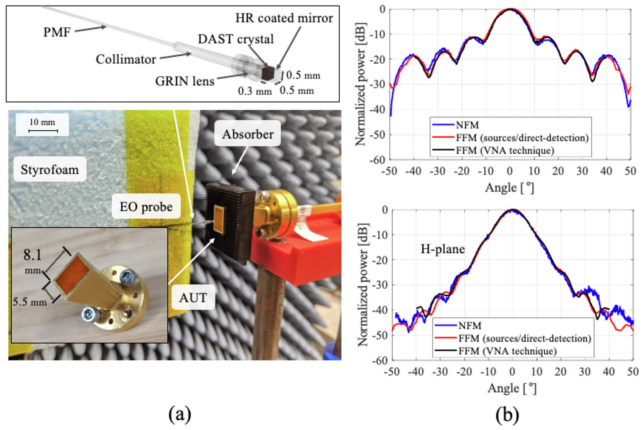

Fig. 1. (a) Photo of the near-field measurement set-up around the AUT. (b) Comparison between NFM and FFMs.

In ThoR, a photonics-based near-field measurement technique [27] has been developed. The test signal [radio frequency (Rf) signal] and reference signal for the measurement [local oscillator (LO) signal] are generated by beating two independent free-running lasers. The optical beat is converted to an RF signal using a uni-travelling-carrier photodiode (UTC-PD). Although the frequency and phase of the RF signal fluctuate, the system can map not only the near-field amplitude, but also the phase distribution thanks to the self-heterodyne technique [28], [29]. Fig. 1(a) shows a photo of the near-field measurement set-up around the antenna under test (AUT). The amplitude and phase distribution on the antenna surface were measured by scanning an electrooptic (EO) probe developed for this purpose. By conducting near-field to far-field conversion, the far-field pattern (radiation pattern) of the AUT can be evaluated. In the ThoR project, three results were compared; the far-field pattern calculated from the near-field pattern measured by the developed system, the far-field pattern directly measured using the source/direct detection technique, and the far-field pattern directly measured using a vector network analyzer (VNA). Fig. 1 presents a comparison of the three results confirming very good agreement with each other.

V. THz Hardware Development

InGaAs (Indium-Gallium-Arsenide)-channel high-electron-mobility transistor (HEMT) devices provide record noise figures and sufficient output power for the realization of high-performance integrated circuits at THz frequencies. Therefore, in this work, a 35 nm InGaAs metamorphic HEMT (mHEMT) technology [30] with current-gain cutoff frequency f_{T} and power-gain cutoff frequency $f_{\max}$ above 500 GHz and 1000 GHz, respectively, is used for the implementation of the 300 GHz front-end circuits.

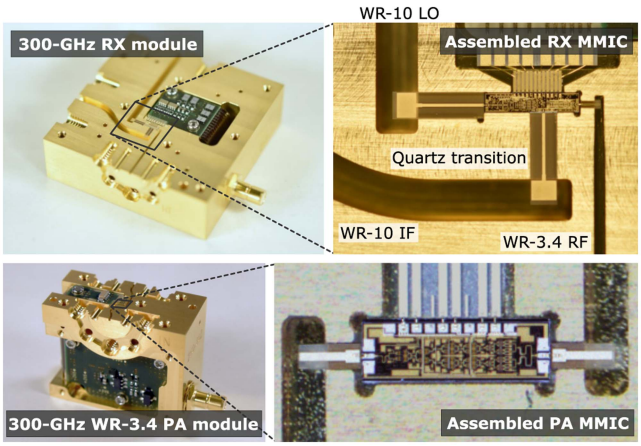

Fig. 2. Photographs of the developed 300 GHz RX and PA modules, showing the lower part of the opened split-block modules as well as a close-up view of the packaged MMICs with waveguide transitions on a quartz substrate.

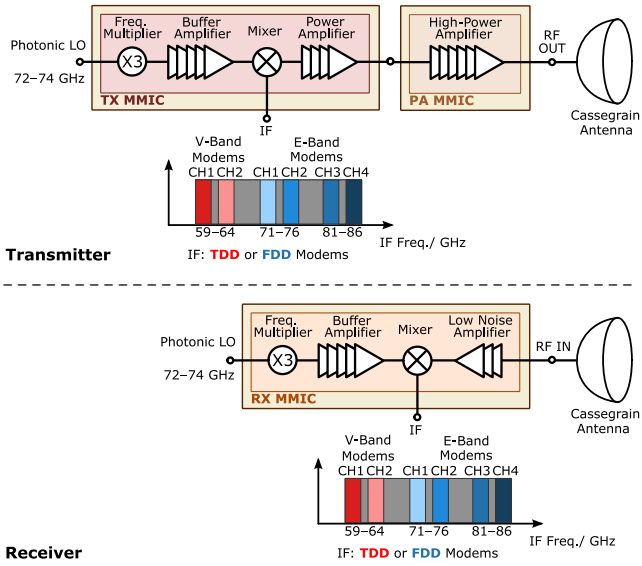

Fig. 3. Overall concept of the ThoR approach.

To implement the real-time capable 300 GHz P2P link described in Section VII, a chipset of multifunctional 300 GHz RX (receiver) and TX (transmitter) millimeter-wave monolithic integrated circuits (MMICs) have been developed. The utilized chipset, including frequency multiplier, amplifier, and mixer circuits, is described in detail in [31] and simplified block diagrams are shown in Fig. 3. In addition, state-of-the-art 300 GHz high-power amplifier MMICs [32] have been developed for the TX side.

The developed 300 GHz MMICs were packaged into waveguide modules to allow easy system integration in a prototype THz link. Photographs of the opened RX and PA (power amplifier) modules are depicted in Fig. 2. Since the developed RX and TX MMICs have the same dimensions and pad configurations, both can be packaged in the same waveguide housing. Also shown are the lower part of the gold-plated brass modules with the assembled 300 GHz circuits as well as the components of the integrated off-chip power supply. The modules are implemented using a split-block packaging technology with E-field-probe-based transitions from the MMICs to the waveguides. The E-field probes are realized on a low-loss quartz substrate and connected via bond wire to the MMICs. With the integrated power conditioning, a bias control, and current sensing of the MMICs is feasible and an external single-supply voltage in the range of 3.3–5 V is sufficient to operate the waveguide modules.

VI. Simulating and Planning of Wireless Backhaul Links

The backhaul link is one of the compelling use cases for THz communications. It serves as an intermediate bridge for data transmission between the central backbone network (core network) and the individual local networks (network edges), whose channel capacity is expected to exceed several hundred Gbps [33]. Typically, backhaul links are provided over fibre connections, which provide a stable channel quality and large channel capacity supporting backhaul requirements. However, fibre is costly and time-consuming to install, which imposes an unpleasant financial burden on mobile network operators (MNOs). In addition, fibre backhaul links are not available everywhere due to geographical issues, legal regulations and administrative restrictions. Therefore, wireless backhaul links have drawn attention as a favorable alternative for MNOs to replace fibre connections providing a relatively inexpensive and fast way to establish the links. The significance of wireless backhaul links is increasing and will continue to grow over the generation of mobile communications, as a greater number of base stations is expected to be deployed to meet the unprecedented demand for high data rates and to provide ubiquitous mobile access for end-user devices.

According to [8], wireless communication using the THz frequency spectrum is capable of supporting fast data transmission (high link capacity) thanks to the large available bandwidth that is sufficient to fulfill the backhaul capacity requirements (several hundred Gbps) even taking into account the unprecedented burgeoning demand for data at mobile nodes.

In [21], the impact of weather conditions on a wireless backhaul link at 300 GHz was researched based on historic weather records, and the corresponding simulation results clearly show the feasibility of the wireless link under real weather conditions. In addition, the simulations of the overall wireless backhaul network across different network architectures, cities, and weather conditions [34], [35], [36], [37], and [38] have demonstrated that multiple wireless backhaul links can be operated reliably under various realistic weather conditions whilst fulfilling backhaul requirements.

However, it is difficult to deploy large numbers of line-of-sight (LOS) THz wireless links with high density in a metropolitan area without interference. ThoR has proposed algorithms for the automatic planning of 300 GHz band wireless fronthaul link deployment in metropolitan areas. Radio wave propagation simulation of wireless fronthaul links was conducted, and the results showed that the SNR signal-to-noise-ratio) and SINR

signal-to-noise-and-interference-ratio) of the automatically deployed 300 GHz band wireless fronthaul links exceeded the required SNR for 100 Gbps data transmission [20], [39]. Moreover, the ThoR project investigated the improvement of the connection ratio of 300 GHz band fronthaul links between remote antenna units (RAUs) and a baseband unit (BBU) during a local downpour by switching routing in a mesh network. A new algorithm for the deployment of RAUs with mesh topology and a route switching algorithm have been developed. It was shown that with mesh topology using the actual rainfall data of Tokyo (Japan) from 2020, THz fronthaul links deployed by these algorithms achieved an annual connection ratio of 99.96 % [19], [20].

VII. ThoR-Hardware Demonstration

The ThoR project was not limited to developing the simulation and planning algorithms or the development and characterization of components described in Sections IV–VI above. To the best of the authors' knowledge, the hardware demonstration realized by the ThoR project is the first bi-directional and real-time-capable demonstration of a 300-GHz P2P link with a real-world-relevant link distance in excess of 100 m, based on a novel super-heterodyne system approach using of-the-shelf E-/V-band modems for base band processing and establishing network connectivity. The overall concept, the characterization of the RF frontend developed in the project, the final set-up and the results achieved are described in the following.

A. Overall Concept

Fig. 3 presents the overall concept of the ThoR approach. Each transmit and receive side uses an E-band local oscillator generated using a photonics-based approach. After frequency tripling to feed an integrated mixer, the IF signal from modems is mixed to create the THz modulated signal, further amplified by an integrated power amplifier and an external high-power amplifier. A Cassegrain reflector is then used as a high-gain antenna, in LOS with the receiver. After the collection of the signal with the second Cassegrain antenna, an integrated LNA is used before the integrated mixer, also fed by the tripled photonic LO. The resulting IF signal is connected to the modems. In the time division duplex (TDD) or frequency division duplex (FDD) demonstration, the system in Fig. 3, this system is doubled, i.e., a pair of Cassegrain antennas is used on each side.

The ThoR FDD link demonstration prototype enables an overall operation bandwidth of 16 GHz within an RF spectrum of approximately 290–310 GHz. This implementation is based on full-duplex FDD operation mode using an IF frequency in E-band (60–90 GHz).

The bandwidth is arranged in four channel pairs, 2 GHz each. The system is capable of up to 32-quadrature amplitude modulation (QAM) spectral efficiency with a target bitrate close to 28 Gbps per direction. The system enhances link throughput by parallelization of multiple lower-throughput modem transceivers. It repurposes affordable commercial E-band modem technology (from Siklu Communications) for a high-throughput 300 GHz link. Siklu EH8010FX is an E-band modem transceiver with an FDD radio operating at 71–76 GHz and 81–86 GHz. Using a symbol rate of 1.6 GHz and a roll-off of 0.25, channels with 2 GHz of bandwidth are formed. In addition, FEC at a FEC rate of 0.87 is added to the data. It features a passive filter for isolation and interference prevention between the two frequency band radios. The radios convert signals to/from RF from/to baseband via an IQ (inphase and quadrature) interface. The modem digitizes and modulates/demodulates the signal into data bits, which a network processor formats into packets for standard networks. An internal processor calibrates the radio and modem for high-order modulation performance.

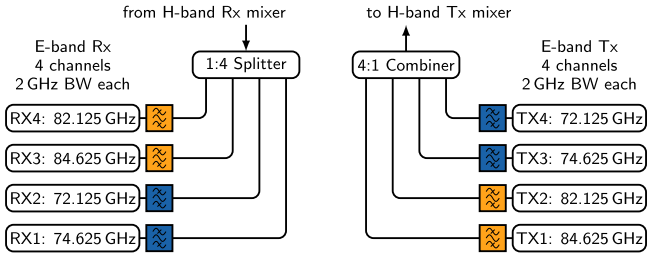

Fig. 4. Bandpass filter for RX/TX isolation. Blue colored is for 71–76 GHz band and yellow colored is for 81–86 GHz band.

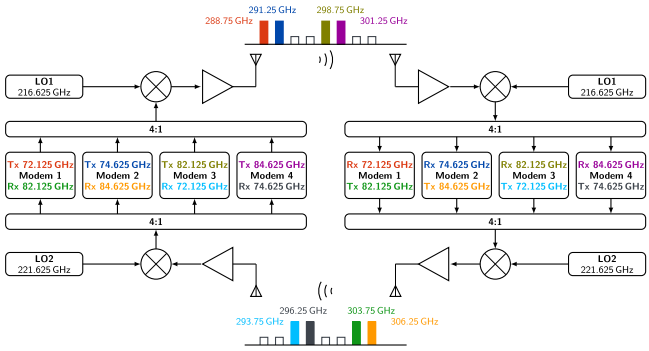

Fig. 5. Full FDD link frequency arrangement.

Using parallel modems with identical IF frequencies can cause interference between IF (intermediate frequency) channels. The prototype design mitigates this by using a band filter for each RX and TX path, as shown in the block diagram in Fig. 4, effectively isolating the receivers from any transmitter-generated interference. The corresponding computer aided design (CAD) model of four modems together with the waveguide-based combiner structure is shown in Fig. 6.

The commercial modem's approach limits IF settings to the regulated E-band frequencies of 71–76 GHz and 81–86 GHz. Only two channels fit in each sub-band, yielding four channels and thus four modems. Fig. 5 shows the frequency arrangement for converting from E-band to a 297.5 GHz-centered operation. It illustrates both ends of the P2P link, each with four FDD modems. Each modem has a TX and RX frequency in either the 71–76 GHz or 81–86 GHz band. The two frequency channels in each band can be combined via a 4:1 combiner for a total of four 2 GHz channels per link direction.

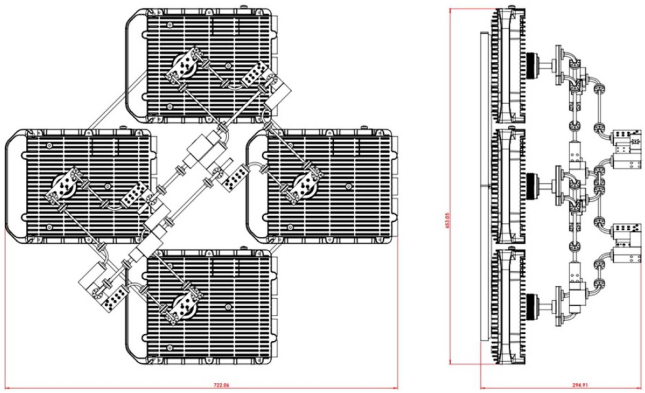

Fig. 6. Mechanical implementation using six two-to-one combiners.

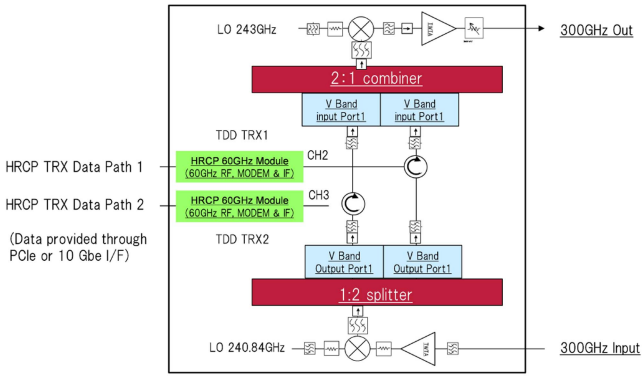

Fig. 7. TDD link configuration using two V-band modems.

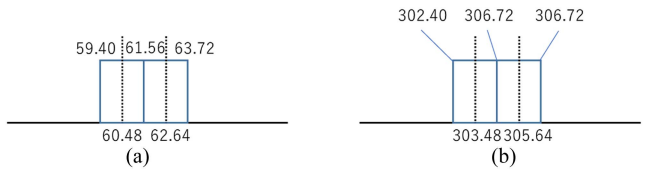

Fig. 8. Channel assignment employed in TDD link. (a) Channel assignment in 60 Hz. (b) Channel assignment in 300 GHz.

The TDD link demonstration utilizes V-band modems to demonstrate the wireless link which is compliant with IEEE Std 802.15.3-2023. The V-band modems within the TDD link have two channels, operating at 59.40–61.56 and 61.56–63.72 GHz, respectively. These 2 GHz channels are up-converted to frequencies around 300 GHz. The TDD link shares the same center frequency channel for both Tx and Rx.

Fig. 7 provides an overview of the TDD link configuration. The V-band modem, developed by HRCP R&D partnership, is capable of achieving a throughput of 6 Gbps using 16-QAM over 2.16 GHz of bandwidth. The V-band modem is compliant with IEEE Std 802.15.3-2023, which covers both V-band and THz with the same PHY/MAC (physical layer/multiple access layer) architecture. Therefore, the upconverted THz signal through the TDD link is also compatible with IEEE Std 802.15.3-2023.

An example of channel assignment within the TDD link is shown in Fig. 8. Once two-channel integration is confirmed to work with this scheme, the total throughput of future terahertz wireless systems can be increased by combining more channels or using higher bandwidth channels.

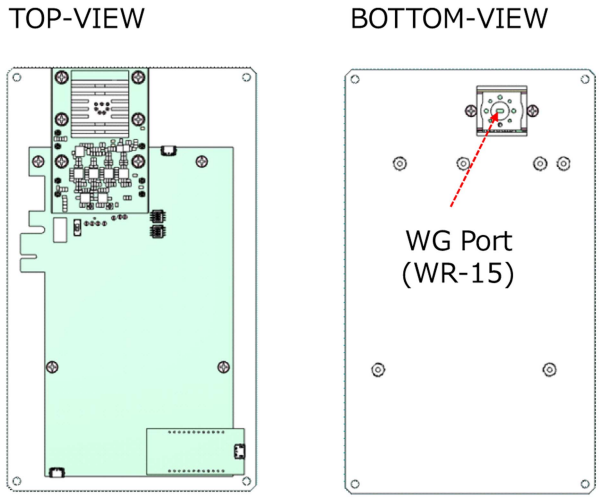

Fig. 9. CAD images of V-band modem.

Fig. 9 shows the CAD images of the V-band modem with a WR-15 port for 60 GHz signal and a peripheral component interconnect express (PCIe) interface for user data transmission, respectively.

B. Characterization of the RF Part

To prepare for the final demonstration of the overall ThoR concept, the novel superheterodyne transmit and receive frontends as well as the high power amplifier (HPA) modules and the photonic LO generation needed to be characterized in great detail.

First, the TX and RX modules were characterized in a back-to-back configuration, and a sensitivity analysis was carried out to find the optimum operating point for different modulation formats, as reported in [40]. sing custom E-band frequency extensions together with an arbitrary-waveform generator (AWG) with up to 25 GHz of bandwidth and a sampling rate of 64 GSa/s as well as a real-time oscilloscope with up to 20 GHz of bandwidth and a sampling rate of 80 GSa/s, which provide and capture the IF signals, data transmissions of up to 32 Gbps using 32-QAM and 8 Gbps using 256-QAM have been demonstrated. Based on measurements of EVM (error vector magnitude) versus Tx IF input power as well as Rx RF input power, the optimum operating points of both modules in terms of TX linearity and RX sensitivity were determined. With the IF input-power sweet spot for the lowest measured EVMrms of the Tx at around −5 dBm and a resulting RF output power of around −8 dBm, the optimum RF input power to the receiver is measured to lie around −024 dBm. This results in a required margin between Tx output and Rx input of 16 dB to enable best signal quality, with a minor dependency on LO and IF frequency combination, as well as the considered modulation schemes quadrature phase shift keying (QPSK), 8-PSK, and 16-QAM.

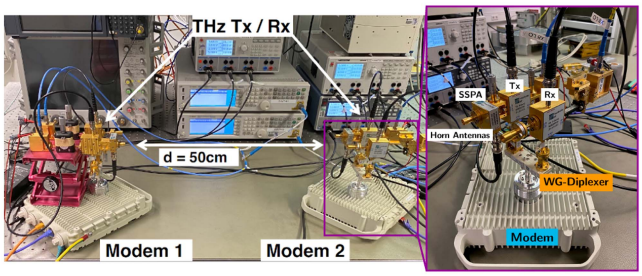

Fig. 10. Laboratory-based link set-up for the first full-duplex real-time wireless link demonstration operating at 300 GHz.

Following the module characterization, a laboratory-based short-range simplex wireless transmission over 1.5 m was carried out as reported in [41]. Using the same E-band frequency extenders as for the module characterization but now connected to baseband modems with a channel bandwidth of 2 GHz and additionally making use of the 300 GHz HPA, the real-time operation of the link was demonstrated achieving a gross data rate of 2.85 Gbps while applying QPSK modulation at a symbol rate of 1.425 Gbps.

By replacing the custom E-band frequency extenders with a set of Siklu E-band modems and mirroring the RF hardware as shown in Fig. 10 to enable bi-directional communication, for the first time a short-range full-duplex real-time wireless link operating in the 300 GHz frequency band in compliance with the IEEE Std 802.15.3d-2017 channel scheme has been demonstrated and reported in [42]. The link proved to operate over 0.5 m using 64-QAM modulation and pushing a total net data throughput of 11.1 Gbps. In addition, the first continuous link operation over 10 h successfully demonstrated the long-term stability of the transmission. The power amplifiers that are used in the link set-up depicted in Fig. 10 provide a typical saturated output power up to 10 dBm, as described in [43]. Before integrating, the PA modules in the TX path, a detailed large-signal characterization was performed to investigate the impairments of the nonlinear behavior of the PA modules for different power levels, which revealed an optimal EVM (error vector magnitude) characteristic for a 16-QAM modulation at 2 dBm output power [44].

The photonic LO architecture is described in Fig. 11. The photonic LO is based on phase modulation of an incoming microwave signal from an electrical source [denoted as Performance Signal Generator (PSG) in Fig. 11], with F_0 frequency. In our case, the synthesizer used is a Rohde & Schwarz SMA100B. Then, an electronic doubler multiplication stage is used, further driving an phase modulator that generates the spectral separation (optical domain) required for the photonic LO. The optical modulated wave is generated from a Keysight 81950 A laser source module. The optical source center frequency is adjusted to the minimum transmission of a fiber grating that has been designed on purpose for this application in the optical telecommunication window around 1550 nm. At its center wavelength, the Bragg grating reflects more than 99% of the incoming light power. The Bragg grating filters out the carrier, thus yielding to an intensity

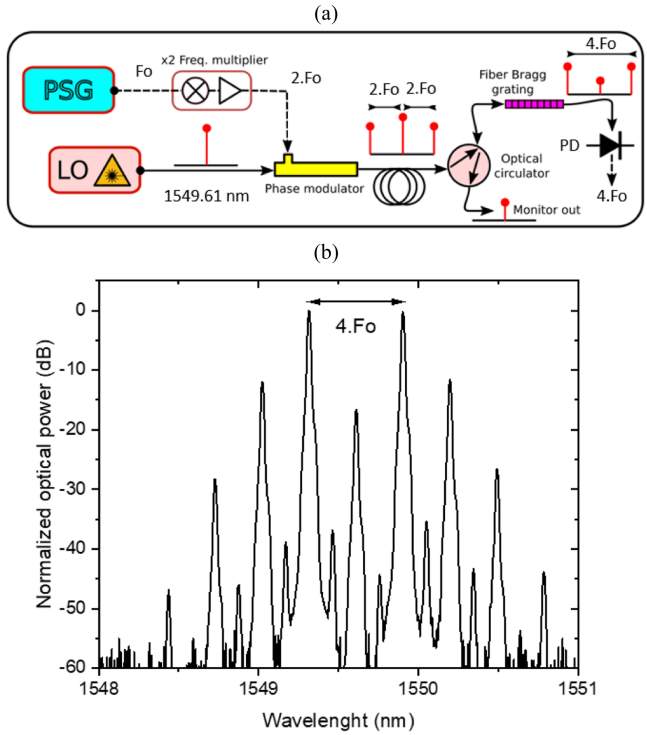

Fig. 11. (a) Architecture of the photonics-based local oscillator (output WR12 amplifier, 3 dB waveguide splitter are not shown). (b) Measured optical spectrum at fiber Bragg grating output, before the PIN-PD.

modulated signal at twice the driving RF (thus at $4{\cdot}F_0$). The full width at minimum of the fiber Bragg grating is 35 GHz with fast roll-off, so that side band attenuation is negligible through it. Finally, a fast PIN photodiode (3 dB bandwidth $\geq$ 70 GHz) converts the optical signal to mm-wave (73.333 GHz in the presented case). An external amplifier (30 dB) is then used, coupled to a 3 dB waveguide splitter to properly drive the Tx and Rx (see Fig. 3) using a set of WR12 flexible waveguides.

The phase noise of F_0 reference and the photonic LO is given in Fig. 12. All of the measured phase noise were obtained using a Rohde and Schwarz FSW67 spectrum analyzer. Considering the architecture of the photonic LO, the phase noise performance is linked to the reference source. The curve (1) of the Fig. 12 is showing the reference phase noise at F_0, and curve (3) is the expected phase noise from a multiplication by 4 [i.e., the phase noise is degraded by 20·log(4) factor]. The measured phase noise of the photonic LO was then done by down-converting the 73.333 GHz with a WR12 sub-harmonic mixer (SHM) pumped at 32 GHz, which phase noise noise is given for reference also (Curve (4), with the factor 20·log(2), as the harmonic 2 is used in the SHM). The curve (2) is showing the photonic LO performance. As shown on Fig. 12, this curve is very close to the multiplication by 4 expected performance, except for offsets range 1–20 kHz. Last, the curve (5) shows the result of an extrapolation of photonic LO multiplied by 3 as per the architecture of the Tx and Rx MMICs (see Fig. 3). The FDD modem specification on phase noise is also shown for reference, and was −90 dBc/Hz @ 1 MHz, highlighting that the performance of the photonic LO (multiplied by 3) is 20 dB

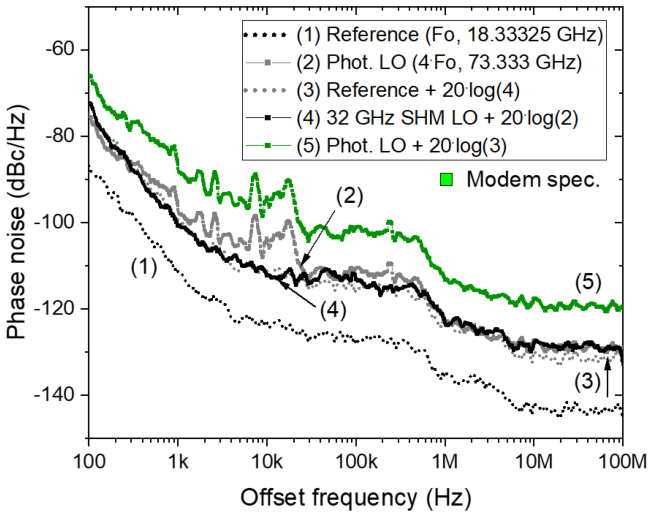

Fig. 12. Measured phase noise of the Photonic LO in the configuration of the outdoor demo of the ThoR project. (1) is the reference RF source used to drive the photonic LO system, and (3) dashed-grey: reference (1) with a 20·log(4) phase noise degradation (x4 frequency multiplication effect). (4) is the phase noise of the SHM local oscillator used to measure the photonic LO phase noise, and (2) is the final phase noise of the photonic LO. (5) is the expected phase noise after being multiplied by 3 (20·log(3) increase), corresponding to the input stages of the Tx and Rx circuits shown in the Fig. 3. The modem requirement is shown for reference in the figure.

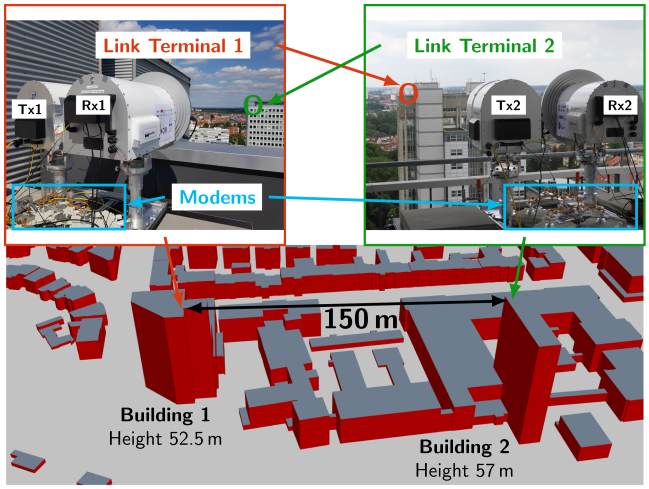

Fig. 13. Link site of the long-range full-duplex link over 150 m and corresponding link terminals 1 and 2.

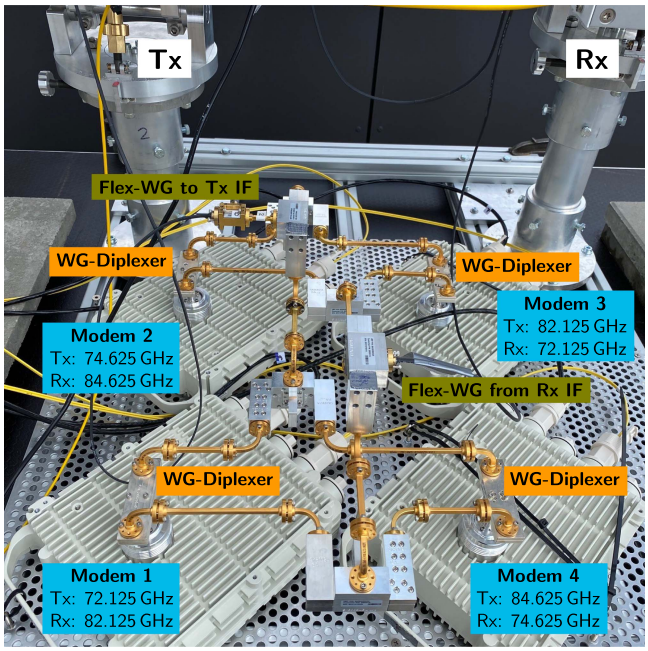

Fig. 14. Aggregation of Siklu modems 1–4 and the diplexing-waveguide structure to separate transmit and receive channels at one of the link terminals.

below the specification for the modems according to the manufacturer. The chosen architecture for the photonic LO enables to reach a phase noise, which is compliant to the requirement of the modem, while being also able to tune the frequency of the LO. The main advantage of this scheme compared to a frequency multiplication approach is that the spectrum is pure, as unwanted harmonics are filtered out by the optical part of the LO system. These harmonics are usually present in pure electronic multiplication stages approaches, leading to the need of an external bandpass filter at the LO output. The use of any filter is moreover a limiting factor when the frequency has to be tuned, which was the case for the THOR approach as the system had to operate with different LO depending on the TDD of FDD Case. The photonic approach thus enabled to tune the frequency of the LO and make it compatible with FDD or TDD, without any bandpass filter inserted between the photonic LO and the transmit or receive circuits.

C. Set-Up of the Final Demo

Based on the results of the characterization of the individual as well as the concatenated RF hardware components and the resulting available link budget, the site for the final demonstration was chosen. Two buildings on the TU Braunschweig campus with heights of 52.6 and 57 m enabled an obstacle-free LOS link over a distance of 150 m, as depicted in Fig. 13. For the outdoor long-range and long-term link demonstrator, the RF hardware was installed in weatherproof and temperature-stabilized antenna housings. For each link terminal, two separate housings for transmitter and receiver were used, with both containing high-gain Cassegrain-antenna systems with an antenna gain of more than 55 dBi, and a half-power beam width of less than 1°. While the TX and HPA modules were housed in the TX antenna, the RX antenna held the RX module as well as the PIN-PD coaxial module (followed by a WR12 amplifier) of the photonic LO. To provide the same LO signal to the TX antenna, the LO is split inside the RX housing and fed to the TX antenna using a flexible WR-12 waveguide interconnection.

The aggregation of four E-band modems at each link terminal is done outside of the antenna housings as depicted in Fig. 14. The connection of the aggregated IF signals with a bandwidth of 4 × 2 GHz in the E-band frequency range to the TX and RX modules inside the antenna housings is done by flexible waveguides. The separation of the individual IF channels of the four modems is achieved with waveguide diplexers, which are described in [42].

TABLE I
SIMULATED ATTENUATION BASED ON REAL WEATHER DATA IN THE PERIOD OF THE EXPERIMENT

	Gaseous attenuation	Rain attenuation	Total attenuation
Max value [dB]	1.8	1.5	2.9
Min value [dB]	0.6	0	0.7
Mean value [dB]	1.2	0.005	1.2
Standard deviation [dB]	0.2	0.067	0.3

To integrate the THz link into a real network, each modem is connected via a SFP+ (small form-factor pluggable) optical fibre transceiver module to a network switch at both ends of the link. From the network switches at both ends of the link the Ethernet signal is transmitted via optical fibre to a central control room, where both data source and sink are located. To evaluate the throughput performance of the link, two PCs in the control room are connected to the network, running open source traffic generation tools serving as server and client in a standard transmission control protocol/Internet Protocol (TCP/IP) communication scenario. At each link terminal, the TX and RX antenna housings have been mounted on a rugged pedestal. Each housing is independently movable in azimuth and elevation by manual adjustment of fine-pitch threads.

Since the response time of the modem graphical user interface (GUI) and the provided link-quality metrics is too slow to perform a precise alignment of the high-gain antennas, additional external hardware was used to adjust the antenna orientation. Using a dielectric-resonator oscillator (DRO) operating at 10.4375 GHz in conjunction with a frequency multiplier (8x) enables the injection of an IF signal at 83.5 GHz into the TX module. Using a similar frequency generation but with a base frequency of 9.1875 GHz as LO source for an E-band down-conversion mixer, the received IF signal at the other link terminal is observed at 10 GHz using a hand-held spectrum analyzer. The alignment is performed by manual iterative scanning of azimuth and elevation of the transmitting and receiving antennas at link terminals 1 and 2, respectively, and simultaneous observation of the received power. This way, up- and down-links are aligned separately.

D. Results of the Final Demonstration

The ThoR demonstration links were set up with the hardware components developed as a part of the project and operated from 7 June 2022 to 30 June 2022. For the demonstrations, two types of duplexing methods (FDD and TDD) were tested using emulated real data in a live operational communication network to assess their practicability for real data transmission.

For the data transmission in the FDD mode, eight commercial FDD modems from Siklu were used to establish two parallel links to emulate a bi-directional link. For each link, four FDD Siklu modems were combined to realize a total of four bi-directional communication channels (2 GHz bandwidth for each channel) through a waveguide-based combining network visualized in Fig. 14.

During the ThoR demonstration, each of the eight individual modem channels, a 2 GHz bandwidth for each, was able to exceed the modem-defined lower CINR (carrier-to-interference-and-noise-ratio) threshold of 16 dB for 16-QAM modulation (4 bps/Hz), yielding a net data rate of 5 Gbps per channel. With the CINR values of the individual modem up- and down-link channels ranging from 17 to 19 dB, none of the duplex channels established by one of the modem pairs sufficiently surpassed the lower CINR threshold for 32-QAM of 19 dB. Taking into account four communication channels for each parallel link, the ThoR demonstration links could showcase a remarkable achievement of 2×20 Gbps net throughput over the sub-mm radio channel around 300 GHz. One thing to note is that the established links were extremely stable, maintaining the 16-QAM scheme constantly throughout the three-week duration of the ThoR demonstration. Only a subtle fluctuation in the received signal strength indicator (RSSI) value of about 1–2 dB was observed resulting in an insignificant drop in CINR value. This subtle variation did not lead to a change in the modulation and coding scheme.

As an additional remark, one communication channel was used for the data streaming channel, which supported the seamless data transmission of live (full high definition) video signal with 50 fps 4:2:2 chroma subsampling.

Apart from the data transmission in the FDD mode, the data transmission in the TDD mode was tested using two TDD modems developed by HRCP using the same set-up of ThoR demonstration hardware. The connection of the data transmission link in the TDD mode was successfully established demonstrating 1 Gbps net throughput. Since the chipsets of the TDD modems already enabled the long RIFS mentioned in Section II the TDD demonstration already complies with IEEE Std 802.15.3-2023.

Besides the measurement, the influence of the atmospheric conditions was investigated using the measured weather parameters measured by a weather station operated by the Leichtweiß-Institute for Hydraulic Engineering and Water Resources at TU Braunschweig. The provided weather data is available for the period of time from 00:00 on 20 June 2022 to 13:00 on 30 June 2022 with the resolution of one minute. Due to the reliability issues of the measurements, a total of 157 431 time slots are considered for the further simulation taking into account two additional attenuation factors were taken into account: attenuation caused by atmospheric gases [45] and attenuation caused by rain [46] for each time slot. The corresponding simulation results about the impact of the atmospheric conditions are given in Table I.

Here, it is possible to observe that the minimum value of the total additional attenuation including gaseous attenuation and rain attenuation is 0.7 dB, and the maximum value is 2.9 dB with the range of 2.2 dB matching closely to the fluctuation value of the RSSI measured by demonstration. A further simulation was carried out on the corner case of heavy rain conditions assuming the rain rate of 100 mm/h to demonstrate the feasibility of the THz communications under the extreme weather conditions and to understand the potential changes in RSSI value for system design. In the worst case (100 mm/h), the rain attenuation corresponds to 4.8 dB, which is not critical enough to cause the link outage rather than forcing the use of a lower

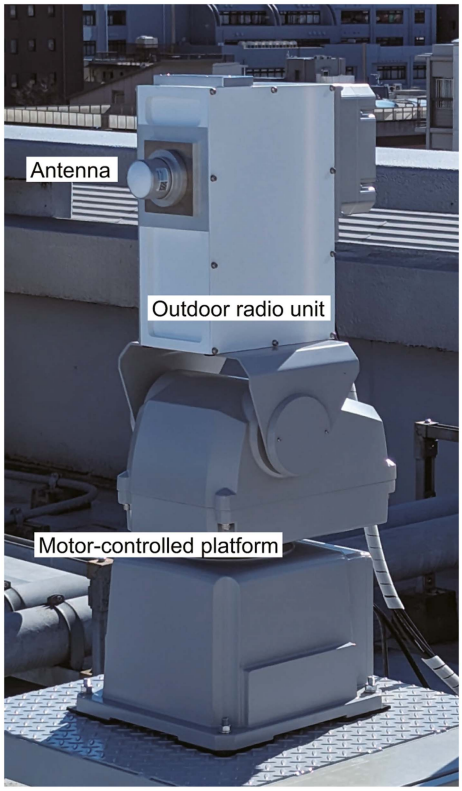

Fig. 15. Outdoor radio unit mounted on a motor-controlled platform.

modulation and coding scheme, which degrades the spectral efficiency of the frequency and thus the lower data transmission rate. This supports the strong evidence for the feasibility of THz communications in the outdoor scenario and the changes in the atmospheric conditions may not be critical enough to hinder THz communications as long as the link distance is properly considered.

VIII. Conclusion

This contribution provides a short introduction to THz communications, taking as an example the application of wireless backhaul links at 300 GHz. Simulation and planning algorithms for THz backhaul links have been briefly described. The core result presented is a hardware demonstrator enabling the proof-of-concept for the realization of the complete system. With this system, a net data rate of 2×20 Gbps over a distance of 150 m using a total bandwidth of 8.64 GHz has been demonstrated showing also compliance with IEEE Std 802.15.3-2023 for this application. In this demonstration, the overall achievable throughput was limited by the base band capabilities of the used modems and a link budget allowing 16-QAM at most. However, this approach can be scaled. Using, e.g., 50 GHz of spectrum instead of 8.6 GHz, two polarizations at the same time and improving the link budget to enable 64-QAM would increase the net throughput by a factor of around 50 yielding a throughput of almost 1 Tbps.

This demonstrator is the basis for further research and development and is currently being used as a starting point in subsequent projects. For example, the EU Horizon Europe project TIMES ("THz Industrial Mesh Networks in Smart Sensing and Propagation Environments") is using parts of the ThoR hardware to demonstrate THz links in industrial environments [47]. Another project, which is based on the findings in ThoR is ongoing in Japan on 300 GHz THz networks, supported by the National Institute of Information and Communications Technology (NICT) under the Beyond 5 G International Joint R&D Program. Based on the TDD mode described in the previous section, waterproof outdoor radio units have been developed for long-term performance evaluation, as shown in Fig. 15. RF output power from a waveguide output port is about 0 dBm and the antenna gain is 40 dBi. The outdoor unit is mounted on a motor-controlled platform for automatic alignment function. IF signals in two IEEE Std 802.15.3e-2017 channels are upconverted into channels 16 and 17 of IEEE Std 802.15.3d-2017, whose frequencies are, respectively, 286.20 and 288.36 GHz. The outdoor radio units will be used in an international collaboration project (Multiphysics based system design for future ICT networks) funded by Japan Science and Technology Agency (JST).

Acknowledgment

The authors would like to thank Simon Haussmann Ivica Bozic, Fiona Woelk, and Sebastian Gottwald to set up the demonstrator, and Christoph Herold who contributed in setting up the software simulations. Guillaume Ducournau would like to thank the IEMN Flagship on Ultra-High datarates (UHD).

References

[1] T. Kürner, D. Mittleman, and T. Nagatsuma, *THz Communciations Paving the Way Toward 1 Tbps*. Berlin, Germany: Springer, 2020.
[2] R. Piesiewicz et al., "Short-range ultra-broadband terahertz communications: Concepts and perspectives," *IEEE Antennas Propag. Mag.*, vol. 49, no. 6, pp. 24–39, Dec. 2007.
[3] T. Kleine-Ostmann and T. Nagatsuma, "A review on terahertz communications research," *J. Infrared Millimeter Terahz Waves*, vol. 32, pp. 173–171, 2011.
[4] S. Koenig et al., "Wireless sub-THz communication system with high data rate," *Nature Photon.*, no. 7, pp. 977–981, 2013.
[5] I. Kallfass et al., "MMIC electronic steerable 4-channel phased-array transmit-receive frontend for 300 GHz wireless personal area networks," in *Proc. 8th Int. Workshop Terahertz Technol. Appl.*, 2018, p. 1.
[6] I. Kallfass, J. Antes, A. Tessmann, T. Zwick, and R. Henneberger, "Multi-gigabit high-range fixed wireless links at high millimeterwave carrier frequencies," in *Proc. IEEE Radio Wireless Symp.*, 2017, pp. 45–48.
[7] C. Castro, R. Elschner, T. Merkle, C. Schubert, and R. Freund, "Experimental demonstrations of high-capacity thz-wireless transmission systems for beyond 5G," *IEEE Commun. Mag.*, vol. 58, no. 11, pp. 41–47, Nov. 2020.
[8] *IEEE Standard for High Data Rate Wireless Multi-Media Networks–Amendment 2: 100 Gb/s Wireless Switched Point-to-Point Physical Layer*, IEEE Standard 802.15.3d-2017 (Amendment to IEEE Standard 802.15.3-2016 as amended by IEEE Standard 802.15.3e-2017), 2017.
[9] T. Kürner and T. Kawanishi, "Demonstrating 300 Ghz wireless backhaul links–The ThoR approach," in *Proc. 47th Int. Conf. Infrared, Millimeter Terahertz Waves*, 2022, pp. 1–1.
[10] ITU-R, *ITU-R Radio Regulations*, vol. 1, Int. Telecommun. Union, 2020. Accessed: Jun. 25, 2024. [Online]. Available: https://www.itu.int/pub/R-REG-RR-2020
[11] ITU -R, *World Radio Comminications Conf. 2023 WRC-23 -Final Acts*, Int. Telecommun. Union, Dec. 2023. Accessed: Jun. 25, 2024. [Online]. Available: https://www.itu.int/pub/R-ACT-WRC

[12] H. Sarieddeen, N. Saeed, T. Y. Al-Naffouri, and M.-S. Alouini, "Next generation terahertz communications: A rendezvous of sensing, imaging, and localization," *IEEE Commun. Mag.*, vol. 58, no. 5, pp. 69–75, May 2020.
[13] ETSI, "Terahertz technology (THz); identification of frequency bands of interest for THz communication systems," ETSI GR THz 002, ETSI ISG, THz, 2024. Accessed: Jun. 25, 2024. Available: https://www.etsi.org/deliver/etsi_gr/THz/001_099/002/01.01.01_60/gr_THz002v010101p.pdf
[14] V. Petrov, T. Kürner, and I. Hosako, "IEEE 802.15.3d: First standardization efforts for sub-terahertz band communications toward 6G," *IEEE Commun. Mag.*, vol. 58, no. 11, pp. 28–33, Nov. 2020.
[15] *IEEE Standard for Wireless Multimedia Networks*, IEEE Standard 802.15.3-2023 (Revision of IEEE Standard 802.15.3-2016), 2023.
[16] T. Kürner, "Terahz–A candidate for 6G; enjoy," *Enjoy – ETSI Mag.*, no. 1, pp. 14–15, 2023. [Online]. Available: https://www.etsi.org/images/files/Magazine/ETSI_Enjoy_MAG_2023_N01_January.pdf
[17] ETSI, "Terahertz technology (THz); identification of use cases for THz communication systems," ETSI GR THz 001, ETSI ISG THz, 2024. Accessed: Jun. 25, 2024. [Online]. Available: https://www.etsi.org/deliver/etsi_gr/THz/001_099/001/01.01.01_60/gr_THz001v010101p.pdf
[18] A. Fricke et al., *IEEE 802.15 document 15-14-0310-19-003d: TG3D channel modelling document (CMD)*, IEEE P802.15 Working Group Wireless Personal Area Netw., 2016. Accessed: Jun. 25, 2024. [Online]. Available: https://mentor.ieee.org/802.15/dcn/14/15-14-0310-19-003d-channel-modeling-document.docx
[19] S. Furukawa, T. Shiraga, R. Okumura, and A. Hirata, "Evaluation of link connectivity ratio of beyond 5G fronthaul wireless links deployed by automatic deployment algorithm during torrential localized rainfall," *IEICE Trans. Commun. (Japanese Ed.)*, vol. J106-B, pp. 760–767, 2023.
[20] A. Hirata and T. Shiraga, "Improvement of line availability of 300-GHz-band wireless fronthaul links during local downpour by switching routing in mesh network," in *Proc. IEEE Int. Symp. Antennas Propag.*, 2023, pp. 1–2.
[21] B. K. Jung and T. Kürner, "Performance analysis of 300 GHz backhaul links using historic weather data," *Adv. Radio Sci.*, vol. 19, pp. 153–163, 2021.
[22] M. Urahashi, R. Okumura, K. Suizu, and A. Hirata, "Complex permittivity evaluation of building materials at 200-500 GHz using THz-TDs," in *Proc. Int. Symp. Antennas Propag.*, 2020, pp. 539–540.
[23] R. Piesiewicz et al., "Scattering analysis for the modeling of THz communication systems," *IEEE Trans. Antennas Propag.*, vol. 55, no. 11, pp. 3002–3009, Nov. 2007.
[24] F. Taleb, G. G. Hernandez-Cardoso, E. Castro-Camus, and M. Koch, "Transmission, reflection, and scattering characterization of building materials for indoor THz communications," *IEEE Trans. THz Sci. Technol.*, vol. 13, no. 5, pp. 421–430, Sep. 2023.
[25] C. Han et al., "Terahertz wireless channels: A holistic survey on measurement, modeling, and analysis," *IEEE Commun. Surveys Tuts.*, vol. 24, no. 3, pp. 1670–1707, Jul./Sep. 2022.
[26] J. Tuovinen, "Method for testing reflector antennas at THz frequencies," *IEEE Antennas Propag. Mag.*, vol. 35, no. 6, pp. 7–13, Dec. 1993.
[27] Y. Tanaka et al., "Photonics-based near-field measurement and far-field characterization for 300-GHz band antenna testing," *IEEE Open J. Antennas Propag.*, vol. 3, pp. 24–31, 2022.
[28] S. Hisatake et al., "Phase-sensitive terahertz self-heterodyne system based on photodiode and low-temperature-grown GaAs photoconductor at 1.55 μm," *IEEE Sensors J.*, vol. 13, no. 1, pp. 31–36, Jan. 2013.
[29] S. Hisatake, H. H. N. Pham, and T. Nagatsuma, "Visualization of the spatial and temporal evolution of continuous electromagnetic waves in the terahertz range based on photonics technology," *Optica*, vol. 1, pp. 365–371, Dec. 2014.
[30] A. Leuther et al.,, "35 nm mHEMT technology for THz and ultra low noise applications," in *Proc. Int. Conf. Indium Phosphide Related Mater.*, vol. 2, pp. 19–20, 2013.
[31] I. Dan et al.,, "A superheterodyne 300 GHz transmit receive chipset for beyond 5G network integration," in *Proc. 16th Eur. Microw. Integr. Circuits Conf.*, 2022, pp. 117–120.
[32] L. John et al., "Broadband 300-GHz power amplifier MMICs in InGaAs mHEMT technology," *IEEE Trans. THz Sci. Technol.*, vol. 10, no. 3, pp. 309–320, May 2020.
[33] B. K. Jung and T. Kürner, "Load analysis of wireless backhaul links at 300 GHz," in *Proc. 48th Int. Conf. Infrared, Millimeter, Terahertz Waves*, 2023, pp. 1–2.
[34] B. K. Jung, N. Dreyer, J. M. Eckhard, and T. Kürner, "Simulation and automatic planning of 300 GHz backhaul links," in *Proc. 44th Int. Conf. Infrared, Millimeter, Terahertz Waves*, 2019, pp. 1–3.
[35] T. Kürner and B. K. Jung, "Automatic planning of nlos backhaul links at 300 GHz arranged in star topology," in *Proc. 24th Gen. Assem. Sci. Symp. Int. Union Radio Sci.*, 2021, pp. 1–3.
[36] B. K. Jung and T. Kürner, "Automatic planning algorithm of 300 GHz backhaul links using ring topology," in *Proc. 15th Eur. Conf. Antennas Propag.*, 2021, pp. 1–5.
[37] B. K. Jung and T. Kürner, "Simulation and automatic planning of NLoS backhaul links at 300 GHz using ring topology," in *Proc. 17th Eur. Conf. Antennas Propag.*, 2023, pp. 1–5.
[38] B. K. Jung and T. Kürner, "Automatic planning algorithms for 300 GHz wireless backhaul links," *IEICE Trans. Commun.*, vol. E105.B, no. 6, pp. 685–693, 2022.
[39] R. Okumura and A. Hirata, "Automatic planning of 300-GHz-band wireless backhaul link deployment in metropolitan area," in *Proc. Int. Symp. Antennas Propag.*, 2021, pp. 541–542.
[40] D. Wrana, L. John, B. Schoch, S. Wagner, and I. Kallfass, "Sensitivity analysis of a 280–312 GHz superheterodyne terahertz link targeting ieee802.15.3 d applications," *IEEE Trans. THz Sci. Technol.*, vol. 12, no. 4, pp. 325–333, Jul. 2022.
[41] D. Wrana, L. John, B. Schoch, S. Wagner, and I. Kallfass, "Short range wireless transmission using a 295–315 GHz superheterodyne link targeting ieee802.15.3 d applications," in *Proc. 51st Eur. Microw. Conf.*, 2022, pp. 205–208.
[42] D. Wrana et al., "Short-range full-duplex real-time wireless terahertz link for ieee802.15.3 d applications," in *Proc. IEEE Radio Wireless Symp.*, 2022, pp. 94–97.
[43] L. John, F. Thome, A. Leuther, and A. Tessmann, "Broadband InGaAs mhemt thz transmitters and receivers," in *Opt. Fiber Commun. Conf.*, 2024, pp. 1–2.
[44] L. John et al., "Non-linear impairments of 300 GHz mpas for thz communications," in *Proc. 47th Int. Conf. Infrared, Millimeter Terahertz Waves*, 2022, pp. 1–2.
[45] ITU-R, *Attenuation by Atmospheric Gases and Related Effects*, Rec. ITU-R P.676-13, International Telecommunications Union, Geneva, Switzerland, Aug. 2022.
[46] ITU-R, *Specific Attenuation Model for Rain for Use in Prediction Methods*, Rec. ITU-R P.838-3, International Telecommunications Union, Geneva, Switzerland, Mar. 2005.
[47] G. Ducournau et al., "Times deliverable D2.3: Definition of scenarios and KPI for hardware demonstration and PoC," Tech. Rep. 6G SNS-TIMES, Sep. 2023.

Thomas Kürner (Fellow, IEEE) received the Dipl.-Ing. degree in electrical engineering, in 1990, and the Dr.-Ing. degree, in 1993, both from the University of Karlsruhe, Karlsruhe, Germany.

From 1990 to 1994, he was with the Institut für Höchstfrequenztechnik und Elektronik (IHE) with the University of Karlsruhe working on wave propagation modeling, radio channel characterization, and radio network planning. From 1994 to 2003, he was with the radio network planning department at the headquarters of the GSM 1800 and UMTS operator E-Plus Mobilfunk GmbH & Co KG, Düsseldorf, where he was team Manager radio network planning support responsible for radio network planning tools, algorithms, processes and parameters from 1999 to 2003. Since 2003, he has been a Full University Professor for Mobile Radio Systems with the Technische Universität Braunschweig.

Dr. Kürner was a Guest Lecturer with Dublin City University within the Telecommunications Graduate Initiative in Ireland, in 2012. Currently, he is chairing the IEEE 802.15 Standing Committee THz and the ETSI Industrial Specification Group THz. He was also the chair of IEEE 802.15.3d TG 100G, which developed the worldwide first wireless communications standard operating at 300 GHz as well as the chair of IEEE 802.15 TG 3mb developing IEEE Std 802.15.3-2023. He was the project coordinator of the H2020-EU-Japan project ThoR ("TeraHertz end-to-end wireless systems supporting ultra-high data Rate applications") and is Coordinator of the German DFG-Research Unit FOR 2863 Meteracom ("Metrology for THz Communications"). In 2019 and 2022, he was a recipient the Neal-Shephard Award of the IEEE Vehicular Technology Society (VTS) and also in 2022 the Best Teacher Award of the European School on Antennas and Propagation (ESoA).

Ralf-Peter Braun received the M.S. and Ph.D. degrees in electrical engineering from the Technical University Berlin, Berlin, Germany, in 1985 and 1995, respectively.

He has more than 40 years of research and industry experience in optical transmission systems and network architectures. After 14 years of research work at the Heinrich-Hertz-Institute, Berlin, he joined Deutsche Telekom in 1997. He setup the Deutsche Telekom SASER R&D TestNet in Germany and supported the setup of the i14y-lab and the T-Labs quantum laboratory at Deutsche Telekom in Berlin. In 2022, he retired and joined the ORBIT Gesellschaft for Application- and Information Systems as a Senior Consultant. Furthermore, he works for the Humboldt University zu Berlin in the field of quantum networks. He is engaged in R&D projects comprising network architecture, technology, service, control, Terahertz communications, visible light communications, test networks, and standardization.

Dr. Braun was a member of VDE, ITG, MEF, and IEEE802.3 working group. Currently he is involved in quantum technologies, including network security, QKD and PQC systems, entanglement swapping, quantum teleportation, and quantum repeaters.

Guillaume Ducournau (Member, IEEE) received the M.Sc. degree from ESIGELEC, Rouen, France, in 2002, and the Ph.D. degree from Université de Rouen, France, 2005.

He has been with the Institute of Electronics, Microelectronics, and Nanotechnology (IEMN), UMR-CNRS 8520, University of Lille, Villeneuve d'Ascq, France, since 2007. He is the Leader of the THz wireless communications activity with IEMN using optoelectronic THz photomixers, electronic receivers, THz instrumentation, and millimeter-wave (mm-wave) characterization. He worked on several European projects: STREP ROOTHz 2010-2013, ThoR H2020, GRAPH-X, TIMES (6 G SNS) as well as the Marie-Curie TERAOPTICS network. At national level, he was the Coordinator of the COM'TONIQ Project from 2014 to 2017 funded by ANR (INFRA 2013) dedicated to THz communications in 300 GHz band, the ANR/DFG TERASONIC project for the use of THz photonics technologies and electrical solid-state technologies for THz communications and SPATIOTERA for spatially distributed photomixers.

Mr. Ducournau was a recipient of the 2020 ISAP BEST PAPER award. He is involved in national France 2030 programs gathering several French laboratories under the "PEPR" programs supported by the ANR (Agence Nationale de la Recherche). In this framework, the FUNTERA project (6 partners) is investigating THz converters, while the SYSTERA project (12 partners) is dedicated to beyond 90 GHz systems for future networks. He also participates to the ST-IEMN common laboratory, and more specifically involved in the mm-wave technologies characterization part. He has authored or co-authored more than 180 publications in peer-reviewed international journals or peer-reviewed conferences proceedings and holds 1 patent.

Uwe Hellrung has been with the Institut für Nachrichtentechnik at Technische Universität Braunschweig, since 1989. In 1996, he received the master craftsman's certificate and since 1997, he is the Head of the precision mechanical workshop with Institut für Nachrichtentechnik. Among his tasks are planning and construction of mechanical platforms and assemblies used in numerous research projects at the institute.

Akihiko Hirata (Senior Member, IEEE) received the B.S. and M.S. degrees in chemistry and the Dr.Eng. degree in electrical and electronics engineering from Tokyo University, Tokyo, Japan, in 1992, 1994, and 2007, respectively.

He joined the Atsugi Electrical Communications Laboratories of Nippon Telegraph and Telephone Corporation (presently NTT Device Technology Laboratories) in Kanagawa, Japan, in 1994. He was a Senior Research Engineer and the Supervisor with NTT Device Technology Laboratories. He has been a Professor with the Chiba Institute of Technology, since 2016. His current research involves millimeter-wave antennas and ultra-broadband millimeter-wave wireless systems.

Dr. Hirata was a recipient of the 2007 Achievement Award presented by the Institute of Electronics, Information, and Communication Engineers (IEICE), the 2008 Maejima Award presented by the Post and Telecom Association of Japan, the 2009 Radio Achievement Award presented by Association of Radio Industries and Businesses Broadcast-Culture, the 2010 Foundation Award presented by the Hoso Bunka Foundation, and the 2011 Commendation for Science and Technology by the Minister of Education, Culture, Sports, Science and Technology. He is a senior member of IEICE.

Shintaro Hisatake (Member, IEEE) received the M.E. and Ph.D degrees in electrical engineering from Doshisha University, Kyoto, Japan in 2000 and 2003, respectively.

From 2003 to 2017, he was an Assistant Professor with the Graduate School of Engineering Science, Osaka University, Osaka, Japan. From 2017 to 2023, he was an Associate Professor and since April 2023, he has been an Full Professor with Gifu University, Gifu, Japan. Since 2021, he has also been a Professor of Industrial Collaboration, Gifu University. Since 2022, his laboratory has been certified as Distinguished Laboratory of Industrial Collaboration. His major fields of research are generation, manipulation, and detection of millimeter- and THz waves based on photonics and their applications.

Prof. Hisatake was a recipient of The Optics Prize for Excellent Papers 2013 from the Japan Society of Applied Physics, in 2014, and the Osaka University Presidential Awards for Encouragement (2014, 2015). In 2016, he was awarded the Young Scientists' Prize of the Commendation for Science and Technology by the Minister of Education, Culture, Sports, Science and Technology, Japan.

Laurenz John received the B.Sc., M.Sc. and Ph.D. (Dr.-Ing) degrees in electrical engineering and information technologies from the Karlsruhe Institute of Technology (KIT), Karlsruhe, Germany, in 2013, 2016, and 2021, respectively.

He is currently a Senior RF/MMIC Design Engineer and Project Leader with Fraunhofer IAF, Freiburg, Germany. Since 2016, he has been involved in the design and characterization of InGaAs-channel HEMT devices and integrated circuits on GaAs and Si substrates for wireless applications up to 800 GHz. His current research interests include IC and package design for radar, communication, and quantum computing applications at mm-wave and THz frequencies.

Bo Kum Jung received the B.E degree in electronic engineering from Inha University, Incheon, South Korea, in 2015, and the M.Sc. degree in electrical engineering from the Technische Universität Braunschweig, Braunschweig, Germany, in 2019. He is currently working toward the Ph.D. degree with the Institut für Nachrichtentechnik at the Technische Universität Braunschweig.

His current research interests include THz communication, mobile network planning, THz propagation channels, and THz X-haul links.

Ingmar Kallfass (Member, IEEE) received the Dipl.-Ing. degree in electrical engineering from the University of Stuttgart, Stuttgart, Germany, in 2000, and the Dr.-Ing. degree in electrical engineering from University of Ulm, Ulm, Germany, in 2005.

In 2001, he worked as a Visiting Researcher with the National University of Ireland, Dublin, Ireland. In 2002, he joined the Department of Electron Devices and Circuits, University of Ulm as a Teaching and Research Assistant. In 2005, he joined the Fraunhofer Institute for Applied Solid-State Physics. From 2009 to 2012, he was a Professor with the Karlsruhe Institute of Technology, Karlsruhe, Germany. Since 2013, he holds the Chair for Robust Power Semiconductor Systems with the University of Stuttgart. His research interests include compound semiconductor-based circuits and systems for power and microwave electronics.

Tetsuya Kawanishi (Fellow, IEEE) received the B.E., M.E., and Ph.D. degrees in electronics from Kyoto University, Kyoto, Japan, in 1992, 1994, and 1997, respectively.

From 1994 to 1995, he was with the Production Engineering Laboratory of Panasonic. During 1997, he was with the Venture Business Laboratory, Kyoto University, where he was engaged in research on electromagnetic scattering and on near-field optics. In 1998, he joined the Communications Research Laboratory, Ministry of Posts and Telecommunications (now the National Institute of Information and Communications Technology, NICT), Tokyo, Japan, where he was the Director of Lightwave Devices Laboratory of NICT. During 2004, he was a Visiting Scholar with the Department of Electrical and Computer Engineering, University of California at San Diego. From 2015, he is a Professor of Faculty of Science and Technology, Waseda University, Tokyo, Japan. His current research interests include high-speed optical modulators, RF photonics and THz communications.

Dr. Kawanishi is the Chair of Task Group on Fixed Wireless Systems and Ground Based Radar Systems (TG-FWS/GBRS) in APT Wireless Group (AWG). From 2017 to 2019, he was a Member of Board of Governors of IEEE Photonics Society. He is currently the President of Electronics Society of IEICE.

Keitarou Kondou received the B.S. degree in physics from Kyoto University, Kyoto, Japan, in 1995, and the M.S. degree in information systems from Nara Institute of Science and Technology, Nara, Japan, in 1997.

He joined Sony Corporation in 1997, focusing on indoor wireless network protocols before moving to signal processing and error-correction technologies for storage and wireless systems. He has participated in IEEE's wireless standardization efforts, focusing on millimeter-wave technology. Since joining the HRCP R&D Partnership in 2017, he has been working on the development of a new wireless System on Chip (SoC) and systems employing millimeter wave technology.

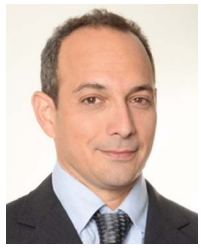

Yigal Leiba received the M.Sc. degree in electrical engineering from the Technion, Haifa, Israel.

He was also a Co-founder and CTO of Breezecom's LMDS group, a spin-off of Breezecom (later Alvarion). His career includes project management and chief Engineer positions at Breezecom, where he was responsible for the development of wireless access and wireless LAN systems. Before Breezecom, he was an R&D Engineer in a technological division with the Israel military-intelligence establishment.

Mr. Leiba is a co-founder and VP R&D of Genopore. Previously he was a co-founder and CTO of Siklu Communication, developing mm-wave backhaul systems. In previous positions, he worked for Runcom Technologies, in charge of the design and the development of the world's first mobile-WiMAX (802.16e) chip, and a voting member of the IEEE 802.16 standard committee.

Bruce Napier received the B.Sc. (*Hons.*) degree in physics from Loughborough University of Technology, Loughborough, U.K., in 1993, the Ph.D. degree from De Montfort University, Leicester, U.K., in 2018 "doctoral research investigated the writing of ultra-long Bragg gratings in optical fibre for dispersion compensation."

He worked with Nortel Networks as Research Engineer on multiplexing components (Harlow, U.K.) and then on integrated components (Paignton, U.K.) and at Gooch and Housego developing its photonic packaging business unit. Since 2008, he has worked on the management and administration of collaborative research projects, especially EU projects, Vivid Components Germany.

Ran Timar received the B.Sc. degree in electrical engineering from the Technion University, Haifa, Israel, in 1996.

He held the position of Director of PHY Systems at Siklu Communications until its recent acquisition by Ceragon Networks, where he now serves as a Group Leader for PHY Systems. With extensive practical experience in the design of antennas, radar, and communication systems, his expertise lies particularly in the millimeter-wave band. Over the last years, he has led the development of numerous successful radar and communication products in the industry.

Alexandre Renau received the Diplome d'ingénieur degree in electrical engineering from Polytech Lille (Lille University Graduate School of Engineers), Villeneuve d'Ascq, France, in 2022. Since 2022, he is working towards the Ph.D. degree, covering the topics of design and qualification of flexible waveguides operating in the submillimeter frequency bands, up to 220 GHz.

His current research interests include waveguides and their transitions for applications up to 220 GHz.

Dr. Renau is a member of the Institute of Electronics, Microelectronics and Nanotechnology (IEMN). He participated in the H2020 EU-Japan ThoR Project, dedicated to the development of km-range super-heterodyne THz transmission systems, especially on the system-level testing of FDD and TDD performance of the final assembly prior to the demos.

Peter Schlegel received the diploma in electrical engineering (Dipl.-Ing.) from the Technische Universität (TU) Braunschweig, Braunschweig, Germany, in 1994.

He is currently a Research Assistant with the Institut für Nachrichtentechnik, the TU Braunschweig. In addition to several smaller projects, he was active in the DVB-T and DVB-T2 technical planning group for northern Germany. His current research interests focuses on visible light communication. He also works as an IT Manager and system administrator and is responsible for the measurement technology with the Institut für Nachrichtentechnik at TU Braunschweig.

Pascal Szriftgiser received the Ph.D. degree in quantum physics from the Laboratoire Kastler Brossel, University Paris VI (Sorbonne University today), Paris, France, in 1996.

He joined CNRS (Centre National de la Recherche Scientifique) at Laboratory PhLAM (Physique des Lasers Atomes et Molécules), in 1996, as a Researcher. Since 2012, he is CNRS Research Director. From 2014 to 2021, he was the Leader of the Cold Atoms Group and Deputy Director of the Laboratory PhLAM from 2019 to 2021. Since 2021, he is PI of Contrat de Projet Etat Région (CPER) WaveTech@HdF, a consortium that brings together six research laboratories in Hauts-de-France region. He has authored or coauthored 135 publications in peer-reviewed international journals or conference proceedings. His expertise spans from cold atoms physics, quantum chaos, topology and nonlinear optics in optical fibres to high-speed coherent optical communications for THz applications.

Axel Tessmann received the Dipl.-Ing. and Ph.D. degrees in electrical engineering from the University of Karlsruhe, Karlsruhe, Germany, in 1997 and 2006, respectively.

In 1997, he joined the Department of Microelectronics, Fraunhofer Institute for Applied Solid State Physics IAF, Freiburg im Breisgau, Germany, where he is involved in the development of monolithically integrated circuits and subsystems for high-resolution imaging systems and high data rate wireless communication links. He is currently a Group Manager with the Millimeter-Wave Packaging and Subsystem Group, Fraunhofer IAF. His main research areas are the design and packaging of millimeter-wave and submillimeter-wave ICs using high-electron-mobility transistors on GaAs, GaN, and InP as well as circuit simulation, and linear and nonlinear device modeling.

Dominik Wrana (Graduate Student Member, IEEE) received the Master of Science degree in electrical engineering from Reutlingen University, Reutlingen, Germany, in 2019.

Since 2019, he has been with the Institute of Robust Power Semiconductor Systems (ILH), University of Stuttgart, Germany, as a Research and Teaching Assistant. He is involved in the design and characterization of monolithic integrated circuits as well as system-level performance analysis and optimization. His current research focuses on the system- to circuit-level engineering for ultra-broadband wireless communications systems operating at millimeter and sub-millimeter wave frequencies.